

NEW MATHEMATICAL MODEL FOR ELECTROSTATIC STABILITY OF THE CASSIE STATE ON MEMS-BASED PILLARED SURFACE

Ki-Young Song*, Kenichi Morimoto and Yuji Suzuki
The University of Tokyo, Japan

ABSTRACT

A new mathematical model of the collapse of Cassie state of a liquid droplet has been developed incorporating the pinning force under electric fields. The effect of the pitch of MEMS-based pillared surfaces upon the electrostatic stability is systematically investigated for development of high-speed droplet manipulation devices to sustain the Cassie state. Our new model is found to be in good agreement with present experiment results quantitatively, whereas the conventional model fails to reproduce the electrostatic stability.

KEYWORDS: Pillared surface, Superhydrophobicity, Electrostatic stability, Cassie state

INTRODUCTION

Recently, digital microfluidics has received great attention for droplet manipulation by applying electric potentials such as electrowetting on dielectrics (EWOD) [1], liquid dielectrophoresis (L-DEP) [2], and L-DEP on electret (L-DEPOE) [3]. For better manipulation of liquid droplets, a large contact angle (over 150 degree) of a liquid droplet on a solid surface is preferred. A superlyophobic surface (SLS) presents a large contact angle (CA) exhibiting the repellency to both aqueous and organic liquids with low adhesion and low friction. The SLS can be achieved using Si micro pillars [4, 5]. However, the liquid droplet on the pillared surfaces becomes electrically unstable when only small electrical potential is applied. The CA changes irreversibly to below 100 degree, causing permanent collapse of the Cassie state.

In the present study, we investigate the electrical (electrostatic) stability of liquid droplets on MEMS-based pillared surfaces [6] both experimentally and analytically. The effect of the pitch of pillared surface upon the electrostatic stability is systematically examined while keeping the solid fraction of the pillar structure constant at 0.01. We develop a mathematical model for estimating the critical voltage over which the Cassie state cannot be sustained. We highlight the advantage of our new model by comparing the present experiment results with the model prediction.

FABRICATION OF PILLARED STRUCTURE

The present pillared structure is a set of cylindrical posts, characterized by the pillar diameter (D), the pillar height (t), and the pitch between adjacent pillars (p). The solid fraction f_s of a pillared surface is defined as $f_s = \pi D^2/4p^2$. Since the static/dynamic superhydrophobicity has been expedited for smaller p [6], the effect of p on the electrical stability is further examined with constant f_s of 0.01.

The present fabrication process is the same as that in Ref.[6]. In this study, the pillar structure with different height ratios ($t^* = t/p$) were fabricated with deep reactive ion etching (DRIE). Figure 1 shows SEM images of the pillar structures. SEM images were analyzed for obtaining f_s of the fabricated structures. In order to achieve desired f_s , the design value of the pillar diameter for EB lithography process was compensated considering the shrinkage of the feature sizes by the side etch during DRIE and also the thickness of plasma-deposited C_4F_8 hydrophobic layer. As shown in Table 1, the accuracy of the present fabrication for constant f_s is within 7% of designed value of 0.01.

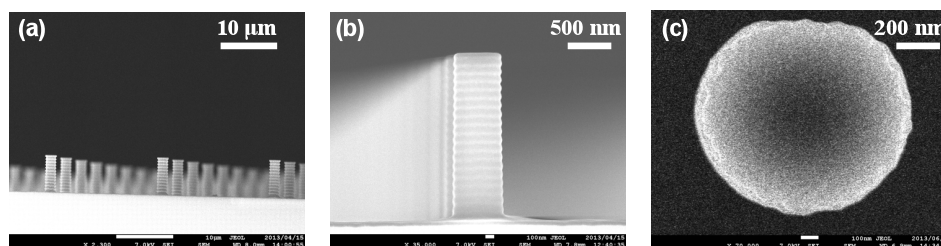


Figure 1: SEM images of fabricated pillar structures after C_4F_8 deposition: (a) a pillar array ($p = 20 \mu\text{m}$, $t^* \sim 0.3$), (b) side view of a pillar ($p = 5 \mu\text{m}$, $t^* \sim 0.3$), and (c) top view of a single pillar ($p = 10 \mu\text{m}$, $t^* \sim 0.3$).

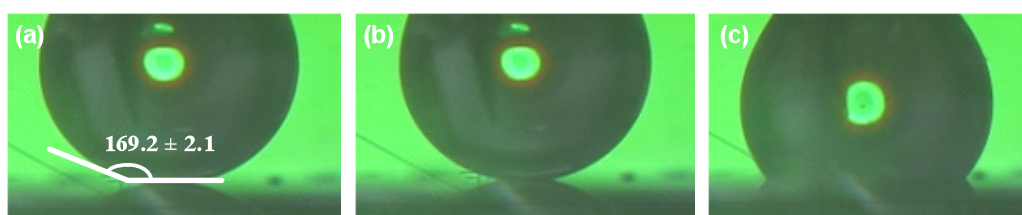


Figure 2: Collapse of a glycerol droplet on a pillared surface ($p = 5 \mu\text{m}$, $t^* \sim 0.3$) induced by electrical potential (V): (a) $V = 0 \text{ V}$, (b) $V = 10 \text{ V}$, and (c) $V = 19 \text{ V}$.

Table 1. Measured f_s values of the present pillar structures with calculated and measured contact angles of a glycerol droplet.

Pitch (μm)	t^*	f_s	CA($^\circ$)	CA ($^\circ$)
		measured	calculated	measured
5	0.1	0.0107 ± 0.0003	171.9	169.1 ± 1.1
	0.3	0.0101 ± 0.0001	172.4	169.2 ± 2.1
	0.5	0.0098 ± 0.0001	172.4	169.7 ± 3.3
10	0.1	0.0104 ± 0.0004	172.0	172.9 ± 1.8
	0.3	0.0101 ± 0.0001	172.0	171.4 ± 1.9
	0.5	0.0098 ± 0.0001	172.0	172.3 ± 2.4
20	0.1	0.0107 ± 0.0002	172.9	169.5 ± 1.4
	0.3	0.0104 ± 0.0001	173.1	169.8 ± 4.6
	0.5	0.0101 ± 0.0001	173.1	169.1 ± 4.0

EXPERIMENTAL

In this study, glycerol with 1% of NH_4Cl was employed as the liquid droplet. We measured the contact angle of the droplets by FACT contact angle meter (CA-D, Kyowa Interface Science Co., LTD.). After the droplet was put onto the pillared surface, electrical potential was applied and gradually increased from 0V to find the minimum voltage with which the droplet collapses as shown in Fig. 2. In the present measurement, in order to stabilize the droplet behavior, the electrical potential was increased with an interval of 1V, keeping the condition for 5 seconds. For one measurement, five samples of the droplets were tested. The contact angles (CAs) and the critical voltages (CVs) for different pitches and heights are summarized in Table 1. It is observed that measured static CA is almost constant regardless of the pitch [6].

MATHEMATICAL MODEL

In order to estimate the critical voltage with which the Cassie-stated-droplet collapses, we have developed a spherical approximation model of a droplet hanging over the pillar array as illustrated in Fig. 3. In this model, the change of the liquid-vapor interface shape is represented by the radius of the approximated sphere, r , the angle of the tangential direction of the sphere from the vertical direction, θ_0 , and the height of the droplet surface from the base substrate, h . Over the spherical surface, three main acting forces were considered: surface tension F_s (upward), pinning force F_p (upward) and electrostatic force F_q (downward) as:

$$F_s = \pi D \gamma_{lv} \cos \theta_0 = \pi D \gamma_{lv} \frac{4(p\sqrt{2} - D)(t - h_0)}{(p\sqrt{2} - D)^2 + 4(t - h_0)^2}, \quad (1)$$

$$F_p = \pi D \gamma_{lv} (\cos \theta_{adv} - \cos \theta_{smooth}), \quad (2)$$

$$F_q = \int_{\theta_0}^{\frac{\pi}{2}} \int_0^{2\pi} \left(-\frac{1}{2} \varepsilon \varepsilon_0 V^2 \right) \frac{r^2}{h^2} \cos \theta \, d\theta \, d\varphi = -\varepsilon \varepsilon_0 V^2 \frac{(p\sqrt{2} - D)^2 + 4(t - h_0)^2}{8th_0}, \quad (3)$$

where γ_{lv} , V , ε , and ε_0 represent the interfacial tension between a liquid and vapor, the applied voltage, the relative permittivity of air, and the permittivity of vacuum, respectively. In Eq.(2), θ_{adv} and θ_{smooth} respectively denote the maximum advancing contact angle and the contact angle on a smooth surface. Both angles were experimentally obtained from non-textured surface. By equating the total force acting on the droplet as $F = F_s + F_p + F_q = 0$, the minimum height (h_0) is obtained as a function of the applied voltage (V) and geometrical parameters of the present pillar structure.

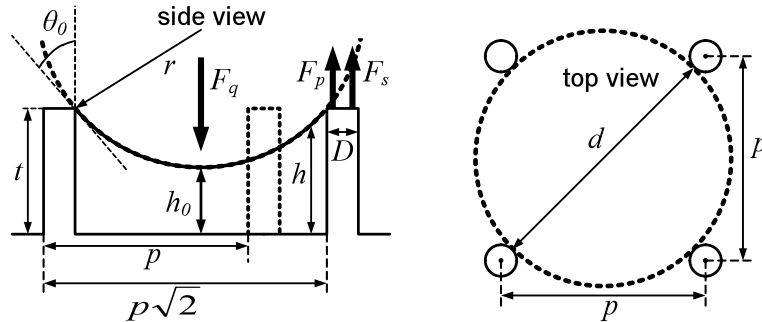


Figure 3: Schematic of a spherical approximation model of a liquid droplet hanging over adjacent pillars.

RESULTS AND DISCUSSION

Figure 4 shows h_0 versus V from three different models: energy-based approach (BG model [7]), present model without the pinning force (Model 0), and present model with the pinning force (Model 1). In the BG model, the critical voltage is obtained through thermodynamic consideration of two extreme energy states: the Cassie state (wetting over the

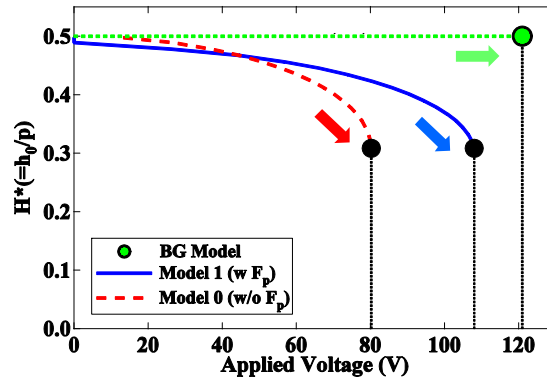


Figure 4: The dependence of the minimum height of the droplet interface on the applied voltage for $p = 20 \mu\text{m}$ and $\tau^* = 0.5$. The black dots correspond to the critical voltage with which the “pull-in” phenomenon occurs for Models 0 & 1.

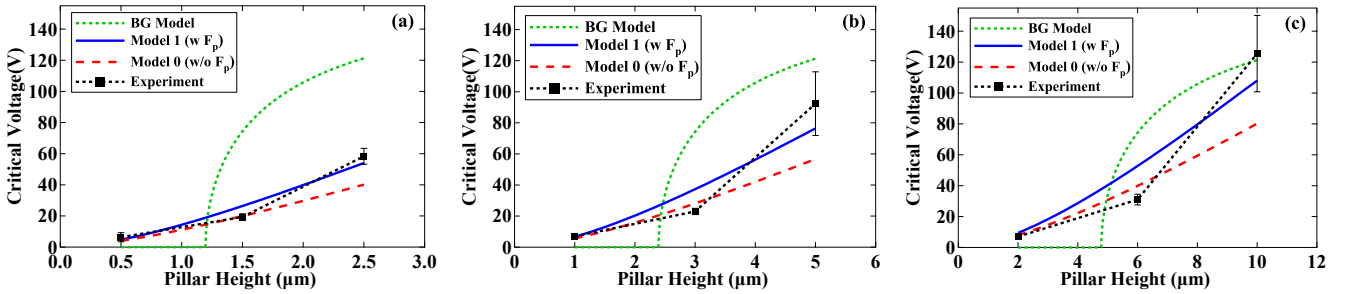


Figure 5: Comparison of the critical voltage versus the pillar height for different pitches: (a) $p = 5 \mu\text{m}$, (b) $p = 10 \mu\text{m}$, and (c) $p = 20 \mu\text{m}$. Model 1 with the pinning force presents the best fit to the experiment results.

pillars) and the Wenzel state (complete wetting over the entire surface). On the other hand, in the present models, the liquid–vapor interface is tracked with increasing the electrostatic force, and the pull-in like phenomena are expressed as in Fig. 4. It is seen that the critical voltage of the present models is smaller than that of BG model. Figure 5 shows the comparison of the model predictions with experiment results. It is seen that the measured CV increases with the pillar height for a constant pitch, and a smaller pitch presents higher CV for a constant pillar height. It is also observed that the present models are in reasonable agreement with experiment results. By considering the pinning force, Model 1 shows better agreement than Model 0. Since the pinning force plays an increasingly dominant role for larger pitches, the discrepancy from the present experiment results is smaller in Model 1 than in Model 0.

However, the BG model exhibits quite different tendency from the present model and fails to reproduce the present experiment results. It is indicated from the over-prediction of the BG model for large pillar heights that the present Cassie state does not transit to complete Wenzel state in the experiments: partial Wenzel state with vapor remained beneath the droplet might be attained after the collapse of the Cassie state.

CONCLUSION

We have developed a new mathematical model for tracking the liquid-vapor interface shape of a droplet, which can describe the collapse of the Cassie state under the electric fields. We fabricated the MEMS-based pillared surfaces keeping the solid fraction constant at 0.01 within 7% accuracy, and examined the effect of the pitch on the electrostatic stability. Unlike the previous energy-based model, the present model incorporating the pinning force can mimic the experiment data of the critical voltage for different pitches.

ACKNOWLEDGEMENTS

The first author acknowledges financial support through Post-doctoral Fellowships for Foreign Researchers by JSPS.

REFERENCES

- [1] H. Moon et al., J. Appl. Phys., 92, pp. 4080-4087 (2002).
- [2] T. B. Jones et al., J. Appl. Phys., 89, pp. 1441-1448 (2001).
- [3] T. Wu et al., J. Micromech. Microeng., 20, 085043 (2010).
- [4] A. Tuteja et al., Science, 318, pp. 1618-1622(2007).
- [5] T. Wu, and Y. Suzuki, Lab Chip, 11, pp. 3121-3129 (2011).
- [6] K. Morimoto et al., Proc. MicroTAS 2012, pp. 64-66.
- [7] V. Bahadur and S.V. Garimella, Langmuir, 23, pp. 4918-4924 (2007).

CONTACT

*K.-Y. Song: ksong@mesl.t.u-tokyo.ac.jp, Y. Suzuki: ysuzuki@mesl.t.u-tokyo.ac.jp